

DESIGN AND ANALYSIS OF CAM MECHANISM WITH NEGATIVE RADIUS ROLLER-FOLLOWER

Jung-Fa Hsieh
Department of Mechanical Engineering, Far East University, Tainan, Taiwan
E-mail: seznof@cc.feu.edu.tw

Received July 2015, Accepted October 2015
No. 15-CSME-80, E.I.C. Accession 3855

ABSTRACT

This paper presents a simple method for the design and analysis of a cam mechanism with a negative radius roller-follower. In the proposed approach, conjugate surface theory is employed to derive a kinematic model of the cam mechanism. Analytical expressions for the pressure angle and principal curvatures of the cam profile are then derived. Finally, analytical expressions for the angular velocity and angular acceleration of the roller are derived. The validity of the proposed design methodology is demonstrated by machining a cam mechanism having a negative radius roller-follower with a radius of 100 mm.

Keywords: negative radius roller-follower; pressure angle; principal curvature.

CONCEPTION ET ANALYSE D'UN MÉCANISME À CAME AVEC POUSSOIR À GALET DE VALEUR NÉGATIVE

RÉSUMÉ

Cet article présente une méthode simple pour la conception et l'analyse d'un mécanisme à came avec poussoir à galet de valeur négative. Dans l'approche proposée, la théorie de surface conjuguée est employée pour dériver un modèle cinématique du mécanisme à came. Les expressions analytiques pour l'angle de pression et des courbures principales du profil de la came sont dérivées par la suite. Finalement, les expressions analytiques pour la vitesse angulaire et l'accélération angulaire du poussoir sont dérivées. La validité de la méthodologie proposée est démontrée en usinant un mécanisme à came comportant un poussoir à galet d'un rayon de 100 mm.

Mots-clés : poussoir à galet d'un rayon de valeur négative; angle de pression; courbure principale.

NOMENCLATURE

$(xyz)_0$	configuration of frame $(xyz)_0$ built in Geneva wheel
${}^0\mathbf{S}$	curved slot surface
${}^r\mathbf{S}$	roller surface
${}^0\mathbf{n}$	unit outward normal of slot surface
R	roller radius
r_b	base circle radius of cam
r	local curvature radius of cam
h	lift height of follower
ψ	pressure angle
θ_1	rotation angle of cam
w_1	angular speed of cam
w_2	angular speed of roller
ε_2	angular acceleration of roller
s_2	displacement of follower

1. INTRODUCTION

Cam elements have many advantageous features for mechanical transmission systems, including simplicity, reliability, repeatability and a low running noise. Contact pairs comprising a convex cylinder and a concave cylinder have a large contact area, and hence a low contact stress [1]. Thus, cam profiles generally have a convex face, while follower profiles have either a convex face or a flat face. In order to distinguish conventional construct, followers with a concave face are referred to as negative radius followers. Cams with negative radius roller-followers use the inner rings of commercial roller bearings as roller-followers. The use of such mechanisms is particularly valuable in applications where space is at a premium and very high forces are involved. Carra et al. [2] presented a design nomograph and synthesis procedure for finding the suitable combination of parameters to satisfy the specified motion law without under-cutting. Wu et al. [3] compared the contact stress of two disc cam mechanisms with a concave-faced follower and a flat-faced follower, respectively. The results showed that the cam mechanism with a concave-faced follower produced a lower maximum contact stress than that with a common flat-faced follower. Moreover, it was shown that the negative radius roller-follower caused the sliding friction between the cam and the follower to be converted to rolling friction. Lin and Chang [4, 5] proposed the conditions of no-undercutting and contact-retaining of the disc mechanism with negative radius roller follower. Furthermore, they presented the mechanical model of a disc cam mechanism with an offset translating negative radius roller follower and deduced the efficiency expression. Later, the same researchers [6] studied the force-locking and shape-locking conjugate cam mechanisms. They extended the “definite proportion and division point” method to solve the theoretical and the actual contour of the cams with negative radius translating roller. Hidalgo-Martinez et al. [7] applied Bezier curves for designing cams with a follower of negative radius. They proposed a numerical method for optimizing the design of the cam profile using a Bezier ordinate as an optimization parameter.

However, the literature lacks a systematic investigation into the design and analysis of cam mechanisms with negative radius roller-followers. Accordingly, this study presents a simple yet robust methodology for the design and analysis of such mechanisms. The proposed methodology comprises four steps, namely (1) establishing a kinematic model of the cam mechanism, (2) designing the cam profile, (3) analyzing the pressure angle and principal curvatures of the cam, and (4) deriving the kinematic model of the roller-follower.

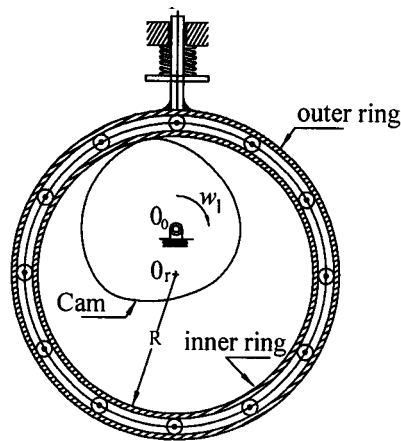


Fig. 1. Cam mechanism with negative radius follower.

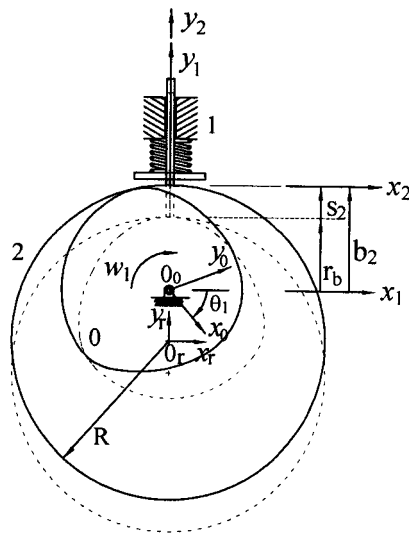


Fig. 2. Simplified representation of cam and follower mechanism for synthesis of cam profile.

2. SURFACE GEOMETRY

In order to analyze the contact stress in a cam mechanism, it is first necessary to determine the profile of the cam. As discussed above, cams with negative radius roller-followers use the inner rings of commercial roller bearings as followers. In other words, the cam fits within an inner ring, as shown in Fig. 1. In synthesizing the cam profile, the cam mechanism can be represented using the simplified model shown in Fig. 2. As shown, the cam rotates with an angular speed w_1 in the clockwise direction about its center point, O_0 . As the cam rotates, the follower rises to a total lift height h over a specified rise angle, remains in a high dwell position over the high dwell angle, falls through a distance h over the return angle, and then remains in a low dwell position over the low dwell angle.

To determine the cam profile using conjugate theory, it is necessary to label all of the coordinate frames in the system, starting with the cam (marked as "0" in Fig. 2) and ending with the translating follower (marked as "2" in Fig. 1). Note that parameter b_2 is defined as $b_2 = r_b + s_2(\theta_1)$, where r_b is the base circle radius of the cam and s_2 is the translating follower displacement.

The configuration of frame $(xyz)_2$ with respect to frame $(xyz)_0$ [8] is given by

$${}^0\mathbf{T} = {}^0\mathbf{T}_1 {}^1\mathbf{T}_2 = \begin{bmatrix} C\theta_1 & -S\theta_1 & 0 \\ S\theta_1 & C\theta_1 & 0 \\ 0 & 0 & 1 \end{bmatrix} \begin{bmatrix} 1 & 0 & 0 \\ 0 & 1 & b_2 \\ 0 & 0 & 1 \end{bmatrix} = \begin{bmatrix} C\theta_1 & -S\theta_1 & -b_2S\theta_1 \\ S\theta_1 & C\theta_1 & b_2C\theta_1 \\ 0 & 0 & 1 \end{bmatrix}, \quad (1)$$

where C and S denote COSINE and SINE, respectively.

To express the surface of the roller in terms of frame $(xyz)_0$, it is first necessary to establish the frame of the roller-follower, namely $(xyz)_r$. The configuration of frame $(xyz)_r$ with respect to frame $(xyz)_2$ is given by the matrix

$${}^2\mathbf{T}_r = \begin{bmatrix} 1 & 0 & 0 \\ 0 & 1 & -R \\ 0 & 0 & 1 \end{bmatrix}, \quad (2)$$

where R is the radius of the roller.

The surface equation, ${}^r\mathbf{S}$, and unit outward normal, ${}^r\mathbf{n}$, of the roller can be expressed with respect to frame $(xyz)_r$ as follows:

$${}^r\mathbf{S} = [RC\theta \quad RS\theta \quad 1]^T, \quad (3)$$

$${}^r\mathbf{n} = [RC\theta \quad RS\theta \quad 0]^T, \quad (4)$$

where θ is the polar angle.

In accordance with the principles of homogeneous coordinate transformation, the cam surface equation, ${}^0\mathbf{S}$, can be expressed as

$${}^0\mathbf{S} = {}^0\mathbf{T}_2 {}^2\mathbf{T}_r {}^r\mathbf{S} = \begin{bmatrix} RC(\theta + \theta_1) + (R - b_2)S\theta_1 \\ RS(\theta + \theta_1) + (b_2 - R)C\theta_1 \\ 1 \end{bmatrix}, \quad (5)$$

In addition, the normal vector, ${}^0\mathbf{n}$, of the cam can be expressed as

$${}^0\mathbf{n} = {}^0\mathbf{T}_2 {}^2\mathbf{T}_r {}^r\mathbf{n} = [C(\theta + \theta_1) \quad S(\theta + \theta_1) \quad 0]^T, \quad (6)$$

Once the input-output relation of the cam mechanism has been defined, the conjugate points and cam profiles can be determined via the formulation

$${}^0\mathbf{n}^T \cdot \frac{d{}^0\mathbf{S}}{dt} = 0, \quad (7)$$

where ${}^0\mathbf{n}$ and ${}^0\mathbf{S}$ are the unit outward normal and surface equation of the cam profile with respect to frame $(xyz)_0$, respectively. The conjugate point (denoted as $\bar{\theta}$) is given by

$$\bar{\theta} = -\tan^{-1}(\bar{F}/\bar{E}), \quad (8)$$

where \bar{E} is defined as $\bar{E} = b_2 - R$ and \bar{F} is defined as $\bar{F} = db_2/d\theta_1$. Substituting Eq. (8) into Eq. (5), the profile of the cam, ${}^0\mathbf{S}$, can be obtained as

$${}^0\mathbf{S} = \begin{bmatrix} RC(\bar{\theta} + \theta_1) + (R - b_2)S\theta_1 \\ RS(\bar{\theta} + \theta_1) + (b_2 - R)C\theta_1 \\ 1 \end{bmatrix}. \quad (9)$$

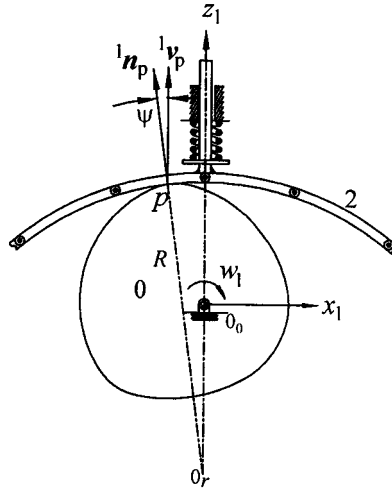


Fig. 3. Pressure angle of cam mechanism with negative radius follower.

3. PRESSURE ANGLE

As shown in Fig. 3, the pressure angle is defined as the angle between the direction of motion (i.e., velocity) of the follower and the direction of the force transmission axis [9]. The pressure angle at the contact point p between the cam and the roller is given by

$$\tan \psi = \frac{\|{}^1\mathbf{n}_p \times {}^1\mathbf{v}_p\|}{|{}^1\mathbf{n}_p \cdot {}^1\mathbf{v}_p|}, \quad (10)$$

where the unit normal vector of the contact point, ${}^1\mathbf{n}_p$, and the direction of velocity of the contact point, ${}^1\mathbf{v}_p$, are both defined with respect to the fixed frame $(xyz)_1$.

The unit normal vector of the contact point on the roller-follower surface with respect to frame $(xyz)_1$ is given by

$${}^1\mathbf{n}_p = {}^1\mathbf{T}_2 {}^2\mathbf{T}_r \mathbf{n}_p = [C\bar{\theta} \quad S\bar{\theta} \quad 0]^T. \quad (11)$$

Meanwhile, the location of the contact point, with respect to frame $(xyz)_1$ is given by

$${}^1\mathbf{S}_p = {}^1\mathbf{T}_2 {}^2\mathbf{T}_r {}^r\mathbf{S} + p = [RC\bar{\theta} \quad RS\bar{\theta} - R + b_2 \quad 1]^T. \quad (12)$$

Since the roller-follower translates along the y_1 axis direction, the direction of velocity of the contact point on the roller-follower surface with respect to frame $(xyz)_1$ can be expressed as

$${}^1\mathbf{v}_p = \frac{d{}^1\mathbf{S}}{dt} = \left[0 \quad \frac{db_2}{dt} \quad 0 \right]^T. \quad (13)$$

Substituting Eqs. (11) and (13) into Eq. (10), the pressure angle, ψ , can be derived as

$$\tan \psi = \frac{\frac{db_2}{d\theta_1}}{R - b_2} = \frac{\frac{db_2}{d\theta_1}}{R - (r_b + s_2)}. \quad (14)$$

Equation (14) shows that an increase of the base circle radius r_b leads to a lower pressure angle ψ . Notably, a higher maximum velocity causes an undesirable increase of the contact pressure angle. However, for negative radius (concave-faced) follower cams, the adverse effects of a higher pressure angle are generally insignificant.

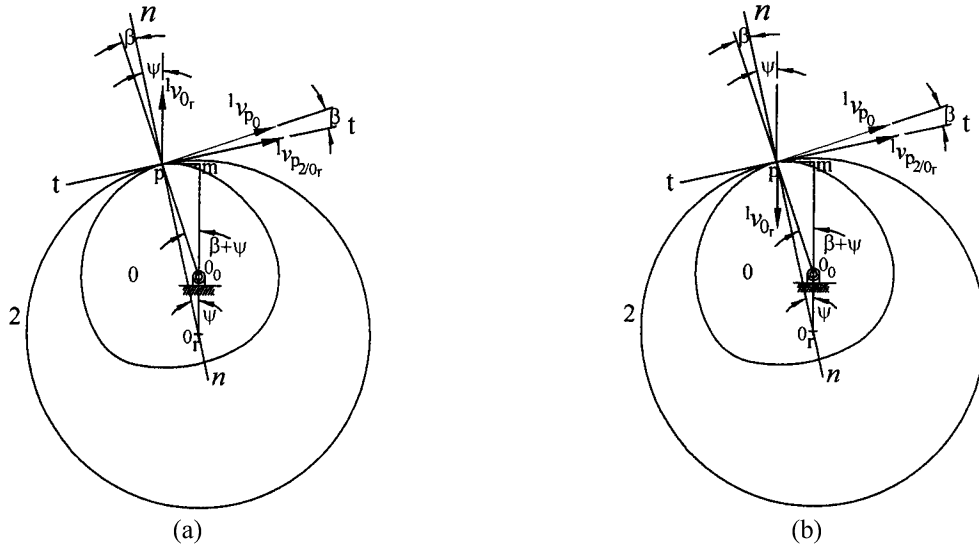


Fig. 4. Kinematic analysis of cam mechanism during: (a) rise of follower and (b) fall of follower.

4. KINEMATIC ANALYSIS

To ensure the contact point between the cam and the roller without sliding in Fig. 1, the cam and roller must share a common tangent vector with the same magnitude at contact point p on the roller-follower surface. Referring to Fig. 4, let directions $n-n$ and $t-t$ represent the common normal vector and common tangent vector for contact point p , respectively. The velocity of contact point p on the follower (denoted as p_2) can be expressed as

$${}^1\mathbf{v}_{p_2} = {}^1\mathbf{v}_{0_r} + {}^1\mathbf{v}_{p_2/0_r}, \quad (15)$$

where ${}^1\mathbf{v}_{0_r}$ is the velocity of the center of the roller and ${}^1\mathbf{v}_{p_2/0_r}$ is the velocity of point p_2 relative to point 0_r .

Similarly, the velocity of contact point p on the cam (denoted as p_0) can be expressed as

$${}^1\mathbf{v}_{p_0} = {}^1\mathbf{v}_{0_0} + {}^1\mathbf{v}_{p_0/0_0} \quad (16)$$

where ${}^1\mathbf{v}_{0_0}$ is the velocity of the origin of the cam and ${}^1\mathbf{v}_{p_0/0_0}$ is the velocity of point p_0 relative to point 0_0 .

For continuous contact to be maintained between the follower and the cam under pure rolling at the contact point, the tangential velocity components of the follower and cam at the contact point should be the same in the rise and fall processes, i.e.,

$${}^1v_{0_r}S\psi + {}^1v_{p_2/0_r} = {}^1v_{p_0}C\beta, \quad (17)$$

$$-{}^1v_{0_r}S\psi + {}^1v_{p_2/0_r} = {}^1v_{p_0}C\beta, \quad (18)$$

where ψ is the pressure angle and β is the angle between ${}^1\mathbf{v}_{p_0}$ and the tangent direction ($t-t$).

From basic kinematic principles, the magnitudes of the two velocities are given as ${}^1v_{p_2/0_r} = R\omega_2$ and ${}^1v_{p_0} = r\omega_1$, respectively. Hence, the roller angular velocities in the rise and fall processes can be expressed respectively as

$$\omega_2 = \frac{r\omega_1 C\beta - {}^1v_{0_r}S\psi}{R}, \quad (19)$$

$$\omega_2 = \frac{r\omega_1 C\beta + {}^1v_{0_r}S\psi}{R}, \quad (20)$$

where r is the local curvature radius of the cam at the contact point and ${}^1v_{0,r} = db_2/d\theta_1 w_1$.

Parameter β in Eqs. (19) and (20) can be derived trigonometrically as

$$\beta = \tan^{-1} \left[\frac{RS\psi}{RC\psi - (R - b_2)} \right] - \psi \quad (21)$$

The roller angular accelerations in the rise and fall processes can then be obtained respectively as

$$\varepsilon_2 = \frac{dw_2}{dt} = \frac{w_1 C \beta \frac{dr}{dt} - r w_1 S \beta \frac{d\beta}{dt} - \frac{d^2 b_2}{d\theta_1^2} w_1^2 S \psi - \frac{d^2 b_2}{d\theta_1^2} w_1 C \psi \frac{d\psi}{dt}}{R}, \quad (22)$$

$$\varepsilon_2 = \frac{dw_2}{dt} = \frac{w_1 C \beta \frac{dr}{dt} - r w_1 S \beta \frac{d\beta}{dt} + \frac{d^2 b_2}{d\theta_1^2} w_1^2 S \psi + \frac{d^2 b_2}{d\theta_1^2} w_1 C \psi \frac{d\psi}{dt}}{R}, \quad (23)$$

where dr/dt , $d\beta/dt$ and $d\psi/dt$ are given in Eqs. (A1–A3) in Appendix A.

5. ANALYSIS OF CURVATURE RADIUS

The curvature radius of the cam must be analyzed in order to prevent the occurrence of singular points. Note that the radius of curvature of the cam cannot be greater than the radius of the follower since unintended multiple-point contacts will otherwise occur [10]. According to basic differential geometry principles, the principal curvatures of the cam profile can be evaluated as follows:

$$K_1, K_2 = H \pm \sqrt{H^2 - K}, \quad (24)$$

where K_1 and K_2 are the principal curvatures, and H and K are defined respectively as

$$K = \frac{LN - M^2}{EG - F^2} \quad \text{and} \quad H = \frac{2FM - EN - GL}{2(EG - F^2)}, \quad (25)$$

where

$$L = {}^0n \cdot \frac{\partial^2 {}^0S}{\partial u^2}, \quad M = {}^0n \cdot \frac{\partial^2 {}^0S}{\partial u \partial \theta_1}, \quad N = {}^0n \cdot \frac{\partial^2 {}^0S}{\partial \theta_1^2}$$

$$E = \frac{\partial {}^0S}{\partial u} \cdot \frac{\partial {}^0S}{\partial u}, \quad F = \frac{\partial {}^0S}{\partial u} \cdot \frac{\partial {}^0S}{\partial \theta_1},$$

and

$$G = \frac{\partial {}^0S}{\partial \theta_1} \cdot \frac{\partial {}^0S}{\partial \theta_1}.$$

(see Eqs. (B1–B6) in Appendix B).

The present study considers the case of a planar cam. Hence, one of the principle curvatures is equal to zero. Moreover, the curvature radius, ρ , of the cam profile is equal to the inverse of the principal curvature

6. IMPLEMENTATION

To validate the design methodology presented in Sections 2–5, a cam mechanism was designed with a negative radius roller-follower having a radius of 100 mm. The motions of the cam and follower were defined by a modified sine motion curve. The follower motion was specified as follows: 20 mm rise for cam rotation from 0 to 150°, dwell for cam rotation to 180°, 20 mm fall for cam rotation to 330°, and dwell for

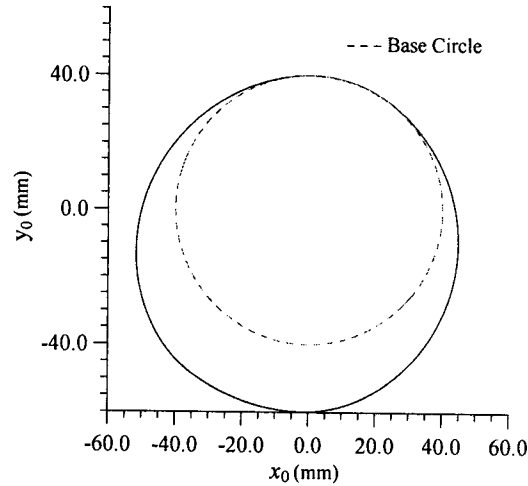


Fig. 5. Simulated profile of cam with negative radius roller-follower.

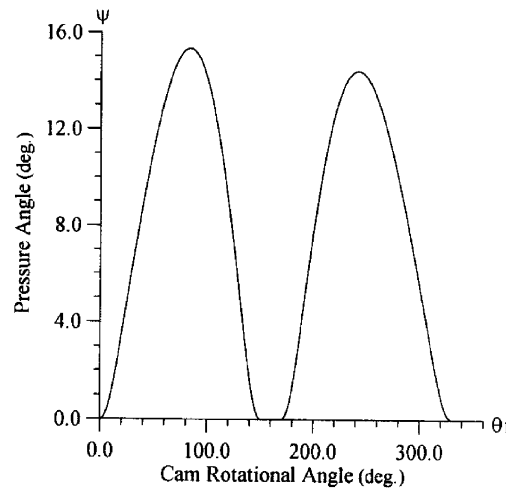


Fig. 6. Variation of pressure angle with cam rotational angle.

the remaining 30° . The radius base circle was specified as 40 mm and the angular speed of the cam was set as $\omega_1 = 10\pi$ rad/s. The modified sine motion curve was specified as shown in Eq. (26), in which θ_1 is the rotational position of the cam, s_2 is the translation displacement of the follower, and θ_d is the dwell period.

$$s_2(\theta_1) = \begin{cases} h \left[\frac{\pi}{4+\pi} \frac{\theta_1 - \theta_d}{\tau} - \frac{1}{4(4+\pi)} S \left(4\pi \frac{\theta_1 - \theta_d}{\tau} \right) \right], & 0 \leq \theta_1 - \theta_d \leq \frac{\tau}{8} \\ h \left[\frac{2}{4+\pi} + \frac{\pi}{4+\pi} \frac{\theta_1 - \theta_d}{\tau} - \frac{9}{4(4+\pi)} S \left(\frac{4\pi}{3} \frac{\theta_1 - \theta_d}{\tau} + \frac{\pi}{3} \right) \right], & \frac{\tau}{8} \leq \theta_1 - \theta_d \leq \frac{7\tau}{8} \\ h \left[\frac{4}{4+\pi} + \frac{\pi}{4+\pi} \frac{\theta_1 - \theta_d}{\tau} - \frac{1}{4(4+\pi)} S \left(4\pi \frac{\theta_1 - \theta_d}{\tau} \right) \right], & \frac{7\tau}{8} \leq \theta_1 - \theta_d \leq \tau \end{cases} \quad (26)$$

Figure 5 shows the simulation results obtained for the cam profile. Figure 6 shows the variation of the pressure angle at the contact point as the cam rotates. Figure 7 shows the curvature radius of the cam profile. Finally, Figs. 8 and 9 show the angular speed and angular acceleration of the roller, respectively.

Figure 10 presents a photograph of the machined cam. Note that the process of generating the NC equations required to produce the driving cam on a 3-axis machine tool is described in [11]. Note also that the

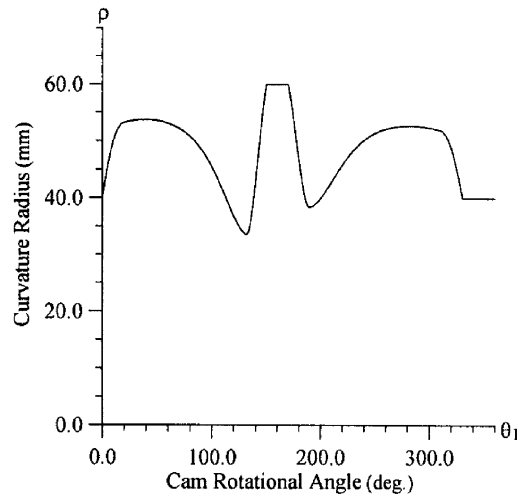


Fig. 7. Variation of curvature radius with cam rotational angle.

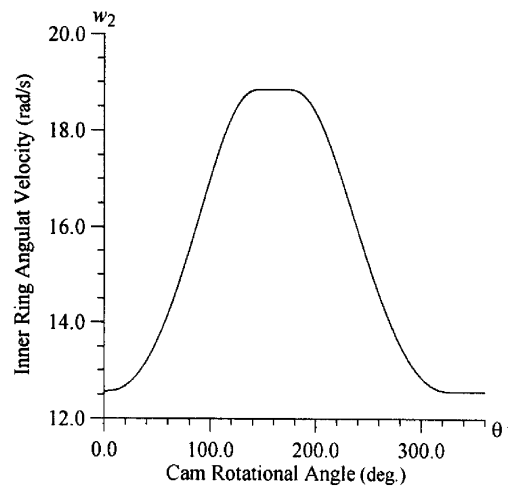


Fig. 8. Variation of angular speed of roller with cam rotational angle.

three holes lying along the x_0 axis of the cam are the workpiece origin (center hole) and clamping holes, respectively. It is seen that a good qualitative agreement exists between the machined profile and the designed profile (see Fig. 5). In addition, Fig. 11 shows the motion simulation of designed cam mechanisms based on CAD software which was found to perform satisfactory. Thus, the feasibility of the proposed methodology is confirmed.

7. CONCLUSIONS

This paper has presented an integrated methodology for the design and analysis of a cam mechanism with a negative radius roller-follower. A kinematic model of the cam mechanism has been derived utilizing the homogeneous coordinate transformation method and conjugate surface theory. In addition, analytical expressions have been presented for the pressure angle and principal curvatures of the cam profile. Finally, a kinematic model has been provided for the case where the roller-follower performs pure rolling at the contact point with the cam. The feasibility of the proposed approach has been demonstrated both numerically and experimentally.

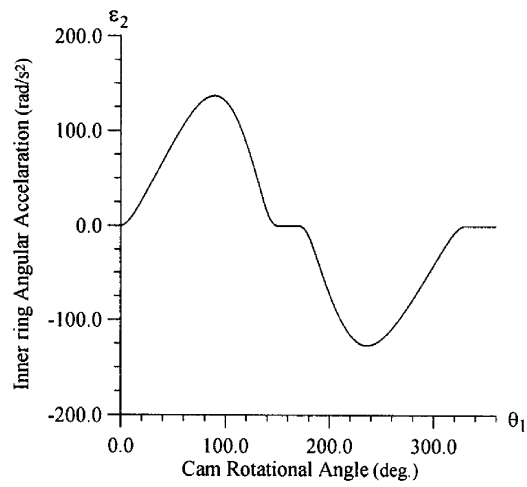


Fig. 9. Variation of angular acceleration of roller with cam rotational angle.



Fig. 10. Photograph of machined cam.

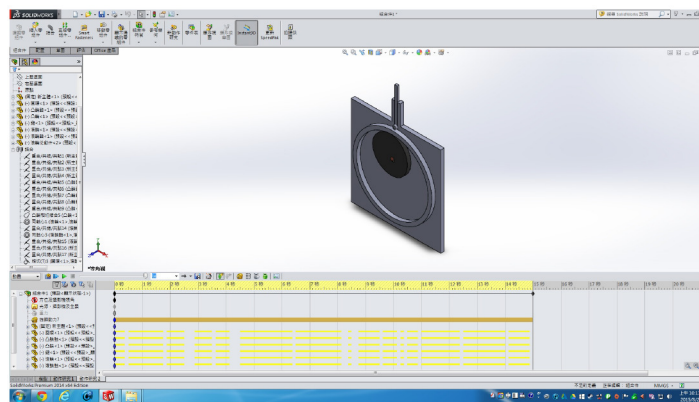


Fig. 11. Motion simulation of designed cam mechanism.

REFERENCES

1. Collins, J.A., *Mechanical Design of Machine Elements and Machines*, John Wiley & Sons Press, New York, 2003.
2. Carra, S., Garziera, R. and Pellegrini, M., “Synthesis of cams with negative radius follower and evaluation of the pressure angle”, *Mechanism and Machine Theory*, Vol. 39, pp. 1017–1032, 2004.
3. Wu, L.-I., Liu, C.-H. and Chen, T.-W., “Disc cam mechanisms with concave-faced followers”, *Proc. Instn. Mech, Part C: J. Mechanical Engineering Science*, Vol. 223, pp. 1443–1448, 2009.
4. Lin, R., Chang, Y., “Mechanical analysis of disc cam mechanisms with negative radius roller translating follower”, *Applied Mechanics and Materials*, Vol. 184–185, pp. 301–306, 2012.
5. Lin, R., Chang, Y., “Optimization design of disc cam mechanisms with an offset translating negative radius roller follower”, *Applied Mechanics and Materials*, Vol. 184–185, pp. 774–779, 2012.
6. Qu, C.L., Chang, Y., “Design of the cam profile with negative radius translating roller follower”, *Applied Mechanics and Materials*, Vol. 470, pp. 412–415, 2014.
7. Hidalgo-Martinez, M., Sanmiguel-Rojias, E. and Burgos M.A., “Design of cams with negative radius follower using Bezier curves”, *Mechanism and Machine Theory*, Vol. 82, pp. 87–96, 2014.
8. McCarthy, J. Michael, *Geometric Design of Linkage*, Springer-Verlag, New York, 2000.
9. Gonzalez-Palacios, M.A. and Angles, J., *Cam Synthesis*, Kluwer Academic Publishers, Dordrecht, 1993.
10. Jones, J. Rees, “Mechanisms-cam curvature and interference”, *Engineering*, Vol. 218(5), pp. 460–463, 1978.
11. Hsieh, Jung-Fa, “Application of homogenous transformation matrix to the design and machining of a Geneva mechanism with curved slots”, *Proc. Instn. Mech. Engrs, Part C: J. Mechanical Engineering Science*, Vol. 221, pp. 1435–1443, 2007.

APPENDIX A

In deriving the angular acceleration of the roller-follower using Eqs. (22) and (23), the related parameter definitions are as follows:

$$\frac{dr}{dt} = \frac{R \frac{db_2}{d\theta_1} w_1 S\bar{\theta} - (R - b_2) \frac{db_2}{d\theta_1} w_1 - R(R - b_2) C\bar{\theta} \frac{d\bar{\theta}}{dt}}{\sqrt{R^2 + (R - b_2)^2 - 2R(R - b_2)S\bar{\theta}}} \quad (1)$$

where

$$\begin{aligned} \frac{d\bar{\theta}}{dt} &= \frac{\left[\left(\frac{db_2}{d\theta_1} \right)^2 - (b_2 - R) \left(\frac{d^2b_2}{d\theta_1^2} \right) \right] w_1}{\left(\frac{db_2}{d\theta_1} \right)^2 + (b_2 - R)^2} \\ \frac{d\psi}{dt} &= \frac{\left[(R - b_2) \frac{d^2b_2}{d\theta_1^2} + \left(\frac{db_2}{d\theta_1} \right)^2 \right] w_1}{(R - b_2)^2 + (db_2/d\theta_1)^2} \\ \frac{d\beta}{dt} &= \frac{R^2 \frac{d\psi}{dt} - (R - b_2) RC\psi \frac{d\psi}{dt} - RS\psi \frac{db_2}{d\theta_1} w_1}{[RC\psi - (R - b_2)0]^2 + (RS\psi)^2} - \frac{d\psi}{dt}. \end{aligned} \quad (2)$$

APPENDIX B

In deriving the principal curvatures of the cam profile using Eqs. (15) and (16), the related parameter definitions are as follows:

$$L = 0, \quad (3)$$

$$M = 0, \quad (4)$$

$$N = -R \left(\frac{d\bar{\theta}}{d\theta_1} + 1 \right)^2 + (R - b_2)S\bar{\theta} - 2C\bar{\theta} \frac{db_2}{d\theta_1} + S\bar{\theta} \frac{d^2b_2}{d\theta_1^2}, \quad (5)$$

$$E = 1, \quad (6)$$

$$F = 0, \quad (7)$$

$$G = R^2 \left(\frac{d\bar{\theta}}{d\theta_1} + 1 \right)^2 + (R - b_2)^2 - 2R(R - b_2)S\bar{\theta} \left(\frac{d\bar{\theta}}{d\theta_1} + 1 \right) + 2RC(\bar{\theta}) \left(\frac{d\bar{\theta}}{d\theta_1} + 1 \right) \frac{db_2}{d\theta_1}, \quad (8)$$

where

$$\frac{d\bar{\theta}}{d\theta_1} = \frac{\left(\frac{db_2}{d\theta_1} \right) \frac{db_2}{d\theta_1} - (b_2 - R) \left(\frac{d^2b_2}{d\theta_1^2} \right)}{(b_2 - R)^2 + \left(\frac{db_2}{d\theta_1} \right)^2}.$$